Inorganic Chemistry

Article

pubs.acs.org/IC

Synthesis and Reversible Transformation of Cu_n-Bridged (n = 1, 2, or 4) Silicodecatungstate Dimers

Kosuke Suzuki, Masahiro Shinoe, and Noritaka Mizuno*

Department of Applied Chemistry, School of Engineering, The University of Tokyo, 7-3-1 Hongo, Bunkyo-ku, Tokyo 113-8656, Japan

Supporting Information

ABSTRACT: Three copper-bridged sandwich-type silicodecatungstate dimers, $TBA_8[Cu(\gamma\text{-}SiW_{10}O_{34})_2(CH_3CONH)_2]\cdot 4H_2O$ (**Cu-1**, TBA = tetra-*n*-butylammonium), $TBA_8H_4[Cu_2(\gamma\text{-}SiW_{10}O_{36})_2H_2O]\cdot 11H_2O\cdot CH_3COCH_3$ (**Cu-2**), and $TBA_8H_2[Cu_4(\gamma\text{-}SiW_{10}O_{36})_2(CH_3COO)_2]\cdot 5H_2O$ (**Cu-4**) have been selectively synthesized by reactions of divacant lacunary $TBA_4[H_4(\gamma\text{-}SiW_{10}O_{36})]$ (SiW10) with copper acetate in organic media. The copper cation(s) in **Cu-1**, **Cu-2**, and **Cu-4** possess square-planar four-coordinate (**Cu-1**), square-pyramidal five-coordinate (**Cu-2**), and octahedral six-coordinate (**Cu-4**) geometries, respectively. These compounds can reversibly be transformed simply by controlling the copper/SiW10 molar ratios in solutions.

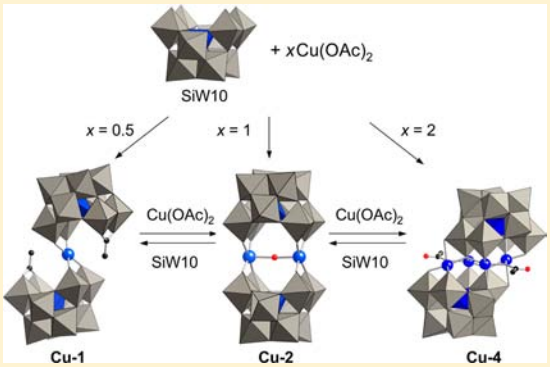

INTRODUCTION

Polyoxometalates (POMs), which are a class of anionic metal–oxygen clusters with large structural versatility, are attractive and useful materials in numerous fields, such as catalysis, medicine, and analytical chemistry, because their chemical and physical properties can be controlled at atomic or molecular levels.[1] Of particular interests are lacunary POMs, which can act as multidentate oxo-ligands by exploiting their variable coordination geometries at the lacunary sites.[2,3]

Reversible structural control of self-assembled coordination architectures in association with changes in coordination geometries and numbers of metal cations leads to switching systems of the functional properties such as redox, magnetism, and catalysis and is of increasing importance.[4] For metal–ligand assembled systems, design of adaptable coordination bonds of metal cations and multidentate ligands is a key to achieve reversible transformation.[4] In this regard, structural control of coordination assemblies can be possible using lacunary POMs. However, reversible transformation of metal-POM assemblies has rarely been reported. To the best of our knowledge, transformation between monomeric and dimeric structures of the only d^0 metal-POM assemblies ($[PTiW_{11}O_{40}]^{5-}$/$[(PTiW_{11}O_{39})_2OH]^{7-}$,[5a] $[\{PW_{11}O_{39}M(\mu\text{-}OH)(H_2O)\}_2]^{8-}$/$[M(PW_{11}O_{39})_2]^{10-}$,[5b] and $[\{P_2W_{17}O_{61}M(\mu\text{-}OH)(H_2O)\}_2]^{14-}$/$[M(P_2W_{17}O_{61})_2]^{16-}$ (M = Hf^{4+} and Zr^{4+})[5c]) has been reported.

Since a copper(II) cation ($S = {}^1/_2$) possesses a flexible and diverse coordination geometry,[6] control of assembled structures with lacunary POMs can be possible. Although various types of copper-containing POMs have been synthesized,[7,8] their reversible structural transformation has never been reported. Recently, we have reported syntheses of metal-containing POMs by reactions of divacant lacunary $TBA_4[H_4(\gamma\text{-}SiW_{10}O_{36})]$ (SiW10, TBA = tetra-*n*-butylammonium)[9] with various metal cations,[10] and these POMs showed catalytic activities for oxidation of alcohol (Zn^{2+}),[10a] hydration of nitrile (Pd^{2+}),[10b] and cyanosilylation of carbonyl compounds (Y^{3+} and Nd^{3+}).[10c,d] Here, we have successfully synthesized three types of copper-bridged silicodecatungstate dimers by reactions of SiW10 with copper acetate ($Cu(OAc)_2$) in organic media. Mono- (**Cu-1**), di- (**Cu-2**), and tetra- (**Cu-4**) nuclear copper cores are sandwiched between two $[\gamma\text{-}SiW_{10}O_{36}]^{8-}$ units and the copper cation(s) in these POMs possess three different coordination geometries. They can reversibly be transformed by changing the copper/SiW10 molar ratios in organic solutions, and their magnetic properties varied with changes in coordination geometries of copper cations (see Figure 1 and Scheme 1).

Scheme 1. Transformations among Cu-1, Cu-2, and Cu-4

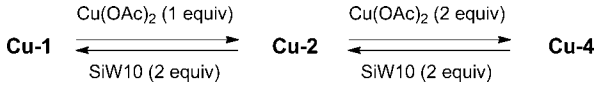

EXPERIMENTAL SECTION

Instruments. IR spectra were measured on Jasco FT/IR-460 Plus using KBr pellets. Thermogravimetric and differential thermal analyses (TG-DTA) were performed on Rigaku Thermo plus TG 8120. Cold-spray ionization mass spectra (CSI-MS) were recorded on JEOL JMS-T100CS. UV–vis spectra were recorded on Jasco V-570 with a Unisoku thermostatic cell holder (USP-230). ^{1}H NMR spectra were measured at 270 MHz on JEOL JNM-EX-270 (internal standard: tetramethylsilane (TMS, $Si(CH_3)_4$)). ICP-AES analyses were performed with Shimadzu

Received: July 10, 2012
Published: October 19, 2012

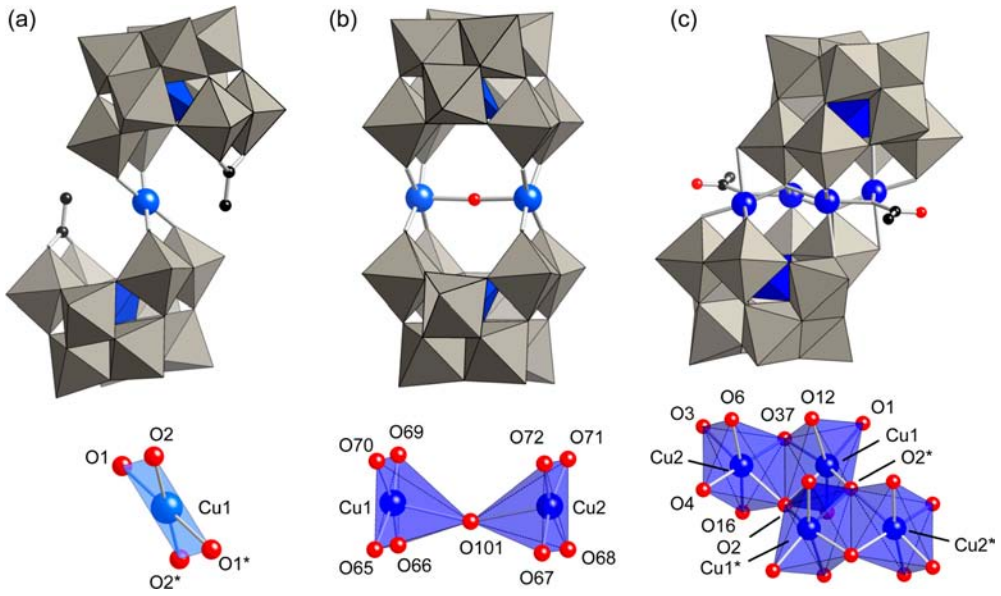

Figure 1. Polyhedral and ball-and-stick representations of the anion parts of (a) **Cu-1**, (b) **Cu-2**, and (c) **Cu-4**. The{WO_6} moieties occupy the gray octahedra, and {SiO_4} groups are shown by internal purple tetrahedra. Blue, red, and black spheres indicate Cu, O, and C atoms, respectively.

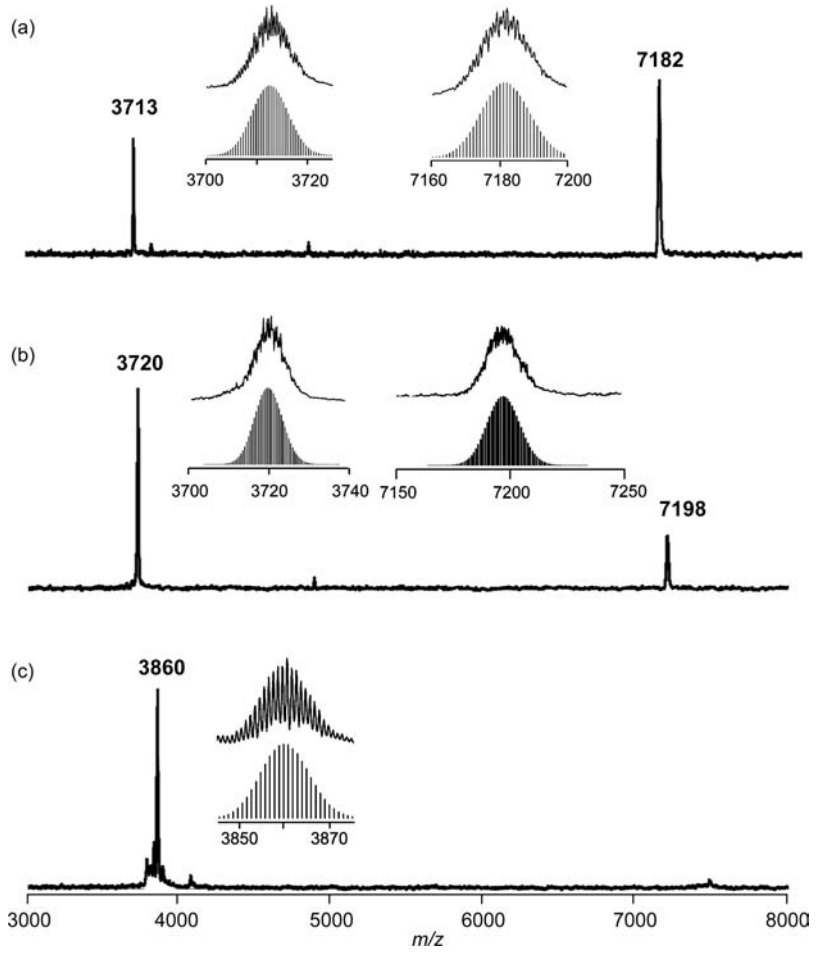

Figure 2. Positive-ion CSI-MS of (a) **Cu-1** (1,2-dichloroethane), (b) **Cu-2** (acetonitrile), and (c) **Cu-4** (acetonitrile). Insets: (a) spectra in the range of m/z 3700−3725 and 7160−7200 and simulated patterns for $[TBA_{10}Cu(SiW_{10}O_{34})_2(CH_3CONH)_2]^{2+}$ (m/z 3713) and $[TBA_9Cu(SiW_{10}O_{34})_2(CH_3CONH)_2]^{+}$ (m/z 7182); (b) spectra in the range of m/z 3700−3740 and 7150−7250 regions and simulated patterns for $[TBA_{10}H_4Cu_2(SiW_{10}O_{36})_2]^{2+}$ (m/z 3720) and $[TBA_9H_4Cu_2(SiW_{10}O_{36})_2]^{+}$ (m/z 7198); (c) spectrum in the range of m/z 3845−3875 and simulated pattern for $[TBA_5H_2Cu_2(SiW_{10}O_{36})(CH_3COO)(OH)]^{+}$ (m/z 3860).

dx.doi.org/10.1021/ic301488a | *Inorg. Chem.* 2012, 51, 11574−11581

Table 1. Crystal Data and Structure Refinement Parameters for Cu-1, Cu-2, and Cu-4

	Cu-1	Cu-2	Cu-4
formula	$C_{147}CuN_{10}O_{75}Si_2W_{20}$	$C_{96}Cu_2N_6O_{73}Si_2W_{20}$	$C_{144}Cu_4N_{14}O_{76}Si_2W_{20}$
formula weight, Fw (g mol^{-1})	6901.29	6265.28	7128.92
cryst syst	monoclinic	monoclinic	monoclinic
space group	$P2_1/n$ (No. 14)	$P2_1$ (No. 4)	$P2_1/n$ (No. 14)
a (Å)	14.6812(2)	18.1007(2)	18.7374(2)
b (Å)	46.9386(4)	26.6281(3)	33.6813(4)
c (Å)	15.7694(2)	22.7005(3)	19.2220(3)
α (deg)	90	90	90
β (deg)	102.2461(7)	89.9710(10)	109.1160(10)
γ (deg)	90	90	90
volume (Å^3)	10619.7(2)	10941.4(2)	11462.1(3)
Z	2	2	2
temp (K)	123(2)	153(2)	153(2)
calculated edensity, ρ_{calcd} (g cm^{-3})	2.158	1.902	2.066
GOF	1.218	1.101	1.123
$R_1{}^a$ [$I > 2\sigma(I)$]	0.0770	0.0707	0.0904
$wR_2{}^a$	0.1638	0.2077	0.2379

$^aR_1 = \sum||F_o| - |F_c||/\sum|F_o|$. $wR_2 = \{\sum[w(F_o^2 - F_c^2)]/\sum[w(F_o^2)^2]\}^{1/2}$.

Table 2. Selected Bond Lengths and Angles for Cu-1, Cu-2, and Cu-4

Cu-1		Cu-2		Cu-4	
		Bond Lengths (Å)			
Cu1−O1	1.927(9)	Cu1···Cu2	4.810(4)	Cu1···Cu2	2.871(3)
Cu1−O2	1.957(10)	Cu1−O65	1.93(2)	Cu1···Cu1*	2.872(4)
		Cu1−O66	1.95(2)	Cu1−O1	1.876(12)
		Cu1−O69	1.90(2)	Cu1−O2	1.950(12)
		Cu1−O70	1.981(19)	Cu1−O2*	1.998(10)
		Cu2−O67	1.95(2)	Cu1−O37	2.007(10)
		Cu2−O68	1.95(2)	Cu1−O12$_{axial}$	2.506(2)
		Cu2−O71	1.93(2)	Cu1−O15$_{axial}$	2.63(1)
		Cu2−O72	2.01(2)	Cu2−O2	1.989(10)
		Cu1−O101	2.44(4)	Cu2−O3	1.955(11)
		Cu2−O101	2.47(4)	Cu2−O4	1.905(13)
				Cu2−O37	1.965(12)
				Cu2−O6$_{axial}$	2.542(2)
				Cu2−O16$_{axial}$	2.46(1)
		Bond Angles (deg)			
O1−Cu1−O2	90.9(4)	Cu1−O101−Cu2	156.5(4)	Cu1−O2−Cu2	93.6(4)
O1−Cu1−O2*	89.1(4)			Cu1−O37−Cu2	92.6(4)
				Cu1−O2−Cu1*	93.3(4)
				Cu1−O2−Cu2*	134.4(6)

ICPS-8100. Magnetic susceptibilities of polycrystalline samples were measured on Quantum Design MPMS-XL7 operating between 1.9 K and 300 K under 1000 Oe magnetic field. Diamagnetic corrections were applied using Pascal constants and diamagnetisms of the sample holder and SiW10.

Materials. Copper acetate was obtained from Kanto Chemical (reagent grade) and used as-received. $TBA_4[H_4(\gamma\text{-}SiW_{10}O_{36})]\cdot H_2O$ (SiW10) was synthesized according to the reported procedure.[9] Acetone, acetonitrile, 1,2-dichloroethane, and diethyl ether were obtained from Kanto Chemical or Aldrich and used as-received.

X-ray Crystallography. Diffraction measurements were made on a Rigaku MicroMax-007 Saturn 724 CCD detector with graphite-monochromated Mo Kα radiation (λ = 0.71069 Å) at 123 or 153 K. The data were collected and processed using CrystalClear[11] for Windows software and HKL2000[12] for Linux software. Neutral scattering factors were obtained from the standard source. In the reduction of data, Lorentz and polarization corrections were made. The structural analyses were performed using CrystalStructure,[13] WinGX,[14] and Yadokari-XG.[15] All structures were solved by SHELXS-97 (direct methods) and refined by SHELXH-97.[16] Metal atoms (Si, W, and Cu) and oxygen atoms in the POM frameworks were refined anisotropically.

Synthesis of $TBA_8[Cu(\gamma\text{-}SiW_{10}O_{34})_2(CH_3CONH)_2]\cdot 4H_2O$ (Cu-1). To an acetone solution (2 mL) of $TBA_4[H_4(\gamma\text{-}SiW_{10}O_{36})]\cdot H_2O$ (100 mg, 29.2 μmol), $Cu(OAc)_2$ (2.90 mg, 14.6 μmol) and acetamide (1.72 mg, 29.2 μmol) were added. The resulting solution was stirred for 10 min at room temperature followed by filtration. The filtrate was kept for one day at 293 K. Pale blue crystals of **Cu-1** suitable for the X-ray crystallographic analysis were obtained (48.6 mg, 48%). ^{1}H NMR (270.5 MHz, DMSO-d_6) δ 0.94 (t, J_2 = 8.12 Hz, 96H, TBA), 1.32 (m, 64H, TBA), 1.58 (m, 64H, TBA), 1.75 (s, acetamide), 3.18 (m, 64H, TBA, 6.66 (s, acetamide), 7.27 (s, acetamide). Elem. Anal.

dx.doi.org/10.1021/ic301488a | Inorg. Chem. 2012, 51, 11574−11581

Calcd (%) for $TBA_8[Cu(SiW_{10}O_{34})_2(CH_3CONH)_2]\cdot 4H_2O$: C, 22.6; H, 4.37; N, 2.00; Si, 0.80; W, 52.4; Cu, 0.91. Found: C, 22.5; H, 4.29; N, 1.86; Si, 0.75; W, 52.1; Cu, 0.86. IR (KBr pellet, cm^{-1}): 1637, 1546, 1483, 1381, 1217, 1153, 1107, 1020, 994, 953, 923, 877, 815, 736, 566, 473, 451, 412, 382, 362, 340, 313, 301. CSI-MS (1,2-dichloroethane): m/z calcd for $[TBA_{10}Cu(SiW_{10}O_{34})_2(CH_3CONH)_2]^{2+}$ 3713, found 3713; calcd for $[TBA_9Cu(SiW_{10}O_{34})_2(CH_3CONH)_2]^{+}$ 7182, found 7182.

Synthesis of $TBA_8H_4[Cu_2(\gamma\text{-}SiW_{10}O_{36})_2H_2O]\cdot 11H_2O\cdot CH_3COCH_3$ (Cu-2). To an acetone solution (8 mL) of $TBA_4[H_4(\gamma\text{-}SiW_{10}O_{36})]\cdot H_2O$ (200 mg, 58.2 μmol), $Cu(OAc)_2$ (11.6 mg, 58.2 μmol) was added. The resulting solution was stirred for 10 min at room temperature, followed by filtration. The filtrate was kept for one day at 293 K. Light blue crystals of **Cu-2** suitable for the X-ray crystallographic analysis were obtained (104 mg, 50%). Elem. Anal. Calcd (%) for $TBA_8H_4[Cu_2(SiW_{10}O_{36})_2H_2O]\cdot 11H_2O\cdot CH_3COCH_3$: C, 21.8; H, 4.44; N, 1.55; Si, 0.78; W, 50.9; Cu, 1.76. Found: C, 21.9; H, 4.27; N, 1.50; Si, 0.71; W, 50.6; Cu, 1.73. IR (KBr pellet, cm^{-1}): 1636, 1483, 1381, 1152, 1093, 1008, 956, 873, 770, 558, 458, 424, 385, 361, 312. CSI-MS (acetonitrile): m/z calcd for $[TBA_{10}H_4Cu_2(SiW_{10}O_{36})_2]^{2+}$ 3720, found 3720; calcd for $[TBA_9H_4Cu_2(SiW_{10}O_{36})_2]^{+}$ 7198, found 7198.

Synthesis of $TBA_8H_2[Cu_4(\gamma\text{-}SiW_{10}O_{36})_2(CH_3COO)_2]\cdot 5H_2O$ (Cu-4). To an acetonitrile solution (1 mL) of $TBA_4[H_4(\gamma\text{-}SiW_{10}O_{36})]\cdot H_2O$ (100 mg, 29.1 μmol), $Cu(OAc)_2$ (11.6 mg, 58.2 μmol) was added. The resulting solution was stirred for 1 h at 293 K followed by filtration. To the filtrate, diethyl ether (2.4 mL) was added and the solution was kept for one day at 293 K. Green crystals of **Cu-4** suitable for the X-ray crystallographic analysis were obtained (62.9 mg, 59%). Elem. Anal. Calcd (%) for $TBA_8H_2[Cu_4(SiW_{10}O_{36})_2(CH_3COO)_2]\cdot 5H_2O$: C, 21.6; H, 4.22; N, 1.55; Si, 0.78; W, 50.9; Cu, 3.52. Found: C, 21.9; H, 4.15; N, 1.55; Si, 0.79; W, 51.1; Cu, 3.45. IR (KBr pellet, cm^{-1}): 1634, 1576, 1484, 1381, 1305, 1152, 1106, 1058, 996, 957, 915, 897, 874, 802, 772, 553, 458, 387, 360, 310. CSI-MS (acetonitrile): m/z calcd for $[TBA_5H_2Cu_2(SiW_{10}O_{36})(CH_3COO)(OH)]^{+}$ 3860, found 3860.

Transformations between Cu-1 and Cu-2. Compound **Cu-1** was transformed to **Cu-2** by addition of 1.0 equiv of $Cu(OAc)_2$ (4.36 mg, 21.8 μmol) to an acetonitrile/water solution (4 mL, 100:1 v/v) of **Cu-1** (153 mg, 21.8 μmol). Compound **Cu-2** was transformed to **Cu-1** by addition of 2.0 equiv of SiW10 (187 mg, 54.5 μmol) to an acetonitrile solution (5 mL) of **Cu-2** (197 mg, 27.3 μmol).

Transformations between Cu-2 and Cu-4. Compound **Cu-2** was transformed to **Cu-4** by addition of 2.0 equiv of $Cu(OAc)_2$ (2.22 mg, 11.1 μmol) to an acetonitrile solution (1 mL) of **Cu-2** (40.0 mg, 5.56 μmol). Compound **Cu-4** was transformed to **Cu-2** by addition of 2.0 equiv of SiW10 (9.42 mg, 2.74 μmol) to an acetonitrile (1 mL) of **Cu-4** (10.0 mg, 1.37 μmol).

RESULTS AND DISCUSSION

Syntheses and Magnetic Properties of Copper-Containing POMs. A mononuclear copper-containing POM (**Cu-1**) was synthesized using acetamide as a capping ligand for two out of four W−O moieties of lacunary sites of $[\gamma\text{-}SiW_{10}O_{36}]^{8-}$, and using the residual two W−O as coordination sites for a copper cation (Figure 1a). Based on this strategy, **Cu-1** was formed by the reaction of SiW10 with 1.0 equiv of acetamide and 0.5 equiv of $Cu(OAc)_2$ in acetone. After one day, single crystals suitable for X-ray crystallographic analysis were successfully obtained. The positive-ion cold-spray ionization mass spectrum (CSI-MS) of the crystals in 1,2-dichloroethane showed only two sets of signals centered at m/z 7182 and 3713 (Figure 2a), which agree well with the patterns calculated for $[TBA_9Cu(SiW_{10}O_{34})_2(CH_3CONH)_2]^{+}$ (m/z 7182) and $[TBA_{10}Cu(SiW_{10}O_{34})_2(CH_3CONH)_2]^{2+}$ (m/z 3713), respectively, indicating formation of a dimeric structure of $[\gamma\text{-}SiW_{10}O_{36}]^{8-}$ units containing one copper cation (Figure 1a). Crystallographic analysis revealed that **Cu-1** was composed of one copper cation and two $[\gamma\text{-}SiW_{10}O_{36}]^{8-}$ units and possessed a "S-shaped" structure, where the copper cation was four-coordinate to four oxygen atoms of lacunary sites of $[\gamma\text{-}SiW_{10}O_{36}]^{8-}$ in a square-planar geometry (Figure 1a, Table 1). The residual W−O moieties at the lacunary sites of $[\gamma\text{-}SiW_{10}O_{36}]^{8-}$ were capped by CH_3CONH.[17]

In contrast to **Cu-1**, dinuclear (**Cu-2**) and tetranuclear (**Cu-4**) copper-containing POMs were synthesized without acetamide and utilized four W−O coordination sites of lacunary sites of $[\gamma\text{-}SiW_{10}O_{36}]^{8-}$. Compounds **Cu-2** and **Cu-4** were selectively obtained using $Cu(OAc)_2$/SiW10 ratios of 1 and 2, respectively. After mixing SiW10 with 1 equiv of $Cu(OAc)_2$ in acetone, light blue single crystals of **Cu-2** suitable for X-ray crystallographic analysis were successfully obtained (50% yield based on SiW10). The CSI-MS in acetonitrile showed two sets of signals centered

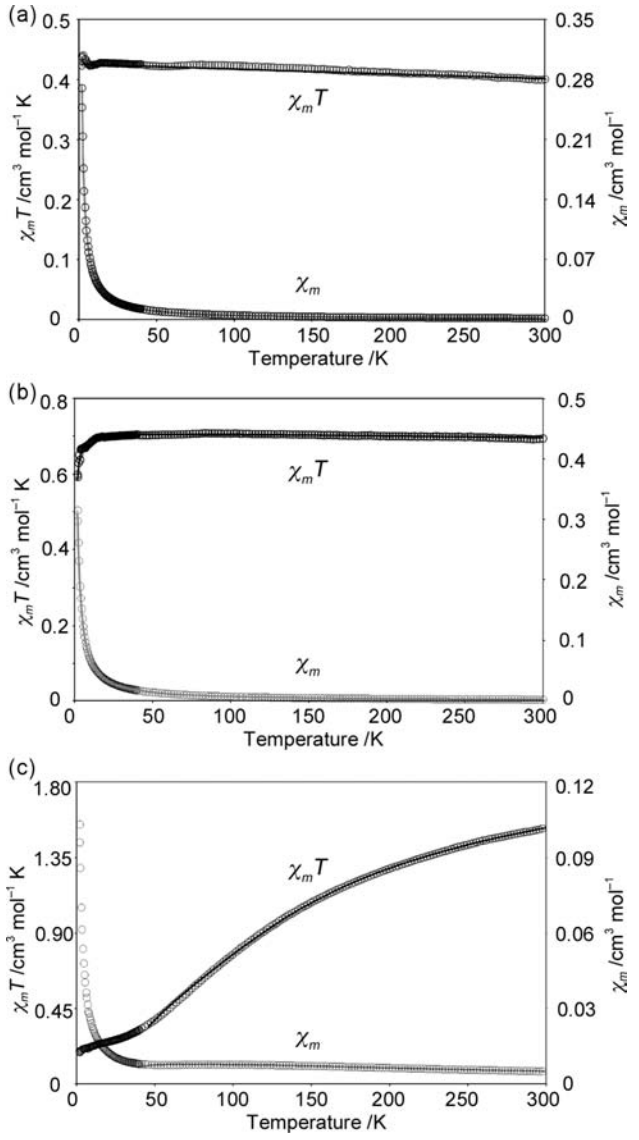

Figure 3. Temperature dependence of χ_m and $\chi_m T$ values of (a) **Cu-1**, (b) **Cu-2**, and (c) **Cu-4** in the temperature range of 1.9−300 K under 1000 Oe field. Solid lines represent the fitting data.

dx.doi.org/10.1021/ic301488a | Inorg. Chem. 2012, 51, 11574−11581

at m/z 7198 and 3720 (Figure 2b), which agree well with the patterns calculated for $[TBA_9H_4Cu_2(SiW_{10}O_{36})_2]^+$ (m/z 7198) and $[TBA_{10}H_4Cu_2(SiW_{10}O_{36})_2]^{2+}$ (m/z 3720), respectively, indicating formation of a dimeric structure of $[\gamma\text{-}SiW_{10}O_{36}]^{8-}$ units with two copper cations. Crystallographic analysis of **Cu-2** revealed that two copper cations were sandwiched by two $[\gamma\text{-}SiW_{10}O_{36}]^{8-}$ units and bridged by one oxygen atom at the axial position (see Figure 1b, Table 1).[18] Each copper cation was five-coordinated to four terminal oxygen atoms of lacunary sites of $[\gamma\text{-}SiW_{10}O_{36}]^{8-}$ (Cu–O bond lengths: 1.90(2)–2.01(2) Å) and one oxygen atom at the axial position (2.44(4) and 2.47(4) Å; see Table 2) in a square-pyramidal geometry. Since the bond valence sum (BVS) value of the axial bridging oxygen atom was 0.24 and low, this oxygen is assignable to a water molecule (aqua ligand). The Cu–O–Cu angle and the Cu···Cu distance were 156.5(4)° and 4.810(4) Å, respectively (Table 2).

Compound **Cu-4** was composed of two $[\gamma\text{-}SiW_{10}O_{36}]^{8-}$ units sandwiching four copper cations, where copper cations were coordinated to $[\gamma\text{-}SiW_{10}O_{36}]^{8-}$ in an "in-pocket" fashion and interacted with the internal $\{SiO_4\}$ tetrahedrons (Figure 1c, Table 1). Each copper cation was six-coordinated to oxygen atoms in elongated octahedral geometries, and the axial Cu–O coordinations were elongated because of the Jahn–Teller distortion (2.46(1)–2.63(1) Å, Figure 1c). Outer two copper atoms (Cu2 and Cu2*) were coordinated to three oxygen atoms of lacunary sites of $[\gamma\text{-}SiW_{10}O_{36}]^{8-}$, one oxygen atom of the acetate ligand, one oxygen atom of the periphery of $[\gamma\text{-}SiW_{10}O_{36}]^{8-}$, and one oxygen atom of the internal $\{SiO_4\}$ tetrahedron. Inner two copper atoms (Cu1 and Cu1*) were coordinated to three oxygen atoms of the lacunary sites of $[\gamma\text{-}SiW_{10}O_{36}]^{8-}$, one oxygen atom of the acetate ligand, and two oxygen atoms of the internal $\{SiO_4\}$ tetrahedrons. Distances and bridging angles between copper cations in **Cu-4** were as follows: Cu1···Cu2 and Cu1···Cu1* distances were 2.871(3) and 2.872(4) Å, respectively; Cu1–O2–Cu2, Cu1–O37–Cu2, Cu1–O2–Cu1*, and Cu1–O2–Cu2* angles were 93.6(4)°, 92.6(4)°, 93.3(4)°, and 134.4(6)°, respectively (Table 2). The IR spectrum of **Cu-4** showed bands at 1576 and 1305 cm^{-1}, assignable to asymmetric and symmetric stretching vibrations of carboxylate groups, respectively.[19] The present $\Delta(\nu_{asym}(COO^-)-\nu_{sym}(COO^-))$ value was 271 cm^{-1} and in the range of those of copper complexes with chelating acetate ligands (240–280 cm^{-1}).[19] The CSI-MS of **Cu-4** in acetonitrile showed a set of signals assignable to the monomerized structure of **Cu-4**, $[TBA_5H_2Cu_2(SiW_{10}O_{36})(OH)(CH_3COO)]^+$ (m/z 3860) (Figure 2c). No set of signals assignable to the dimeric

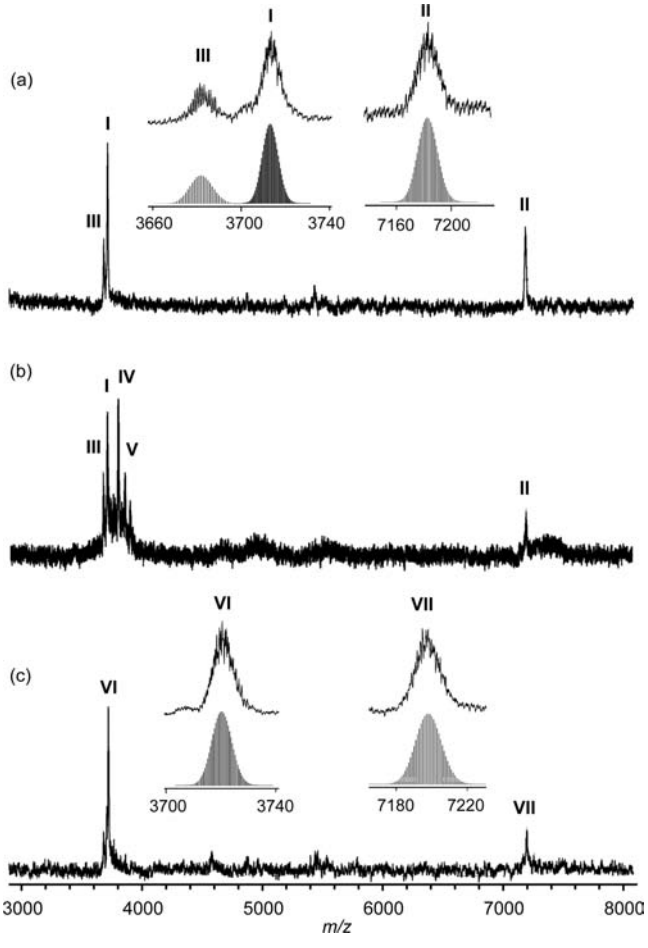

Figure 4. Positive-ion CSI-MS of (a) **Cu-1** (acetonitrile) and **Cu-1** treated with (b) 1 equiv of $Cu(OAc)_2$ (acetonitrile) and (c) 1 equiv of $Cu(OAc)_2$ and water (acetonitrile/water, 100:1 v/v). The signals of **I**, **II**, **III**, **IV**, and **V** are assignable to $[TBA_{10}Cu(SiW_{10}O_{34})_2(CH_3CONH)_2]^{2+}$ (**Cu-1**, m/z 3713, **I**) and $[TBA_9Cu(SiW_{10}O_{34})_2(CH_3CONH)_2]^+$ (**Cu-1**, m/z 7182, **II**), $[TBA_5H(SiW_{10}O_{34})(CH_3CONH)]^+$ (SiW10, m/z 3682, **III**), $[TBA_5Cu(SiW_{10}O_{34})(CH_3CONH)(CH_3COO)]^+$ (m/z 3803, **IV**), $[TBA_5H_2Cu_2(SiW_{10}O_{36})(CH_3COO)(OH)]^+$ (**Cu-4**, m/z 3860, **V**), $[TBA_{10}H_4Cu_2(SiW_{10}O_{36})_2]^{2+}$ (**Cu-2**, m/z 3720, **VI**), $[TBA_9H_4Cu_2(SiW_{10}O_{36})_2]^+$ (**Cu-2**, m/z 7198, **VII**). Insets: observed spectra and simulated patterns.

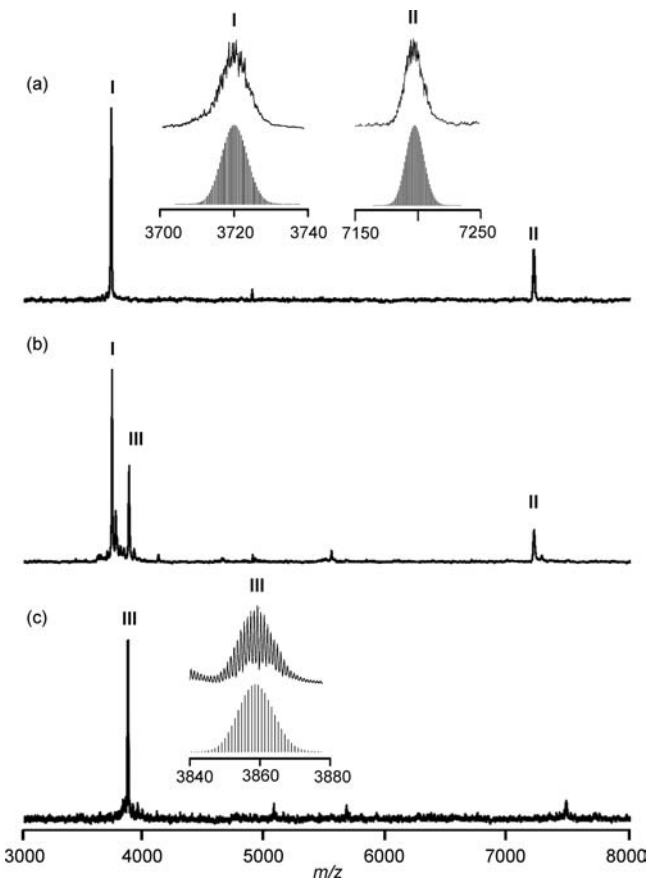

Figure 5. Positive-ion CSI-MS of (a) **Cu-2** and **Cu-2** treated with (b) 0.5 equiv and (c) 2.0 equiv of $Cu(OAc)_2$ (acetonitrile). The signals of **I**, **II**, and **III** are assignable to $[TBA_{10}H_4Cu_2(SiW_{10}O_{36})_2]^{2+}$ (**Cu-2**, m/z 3720, **I**), $[TBA_9H_4Cu_2(SiW_{10}O_{36})_2]^+$ (**Cu-2**, m/z 7198, **II**), and $[TBA_5H_2Cu_2(SiW_{10}O_{36})(CH_3COO)(OH)]^+$ (**Cu-4**, m/z 3860, **III**), respectively. Insets: observed spectra and simulated patterns.

dx.doi.org/10.1021/ic301488a | Inorg. Chem. 2012, 51, 11574–11581

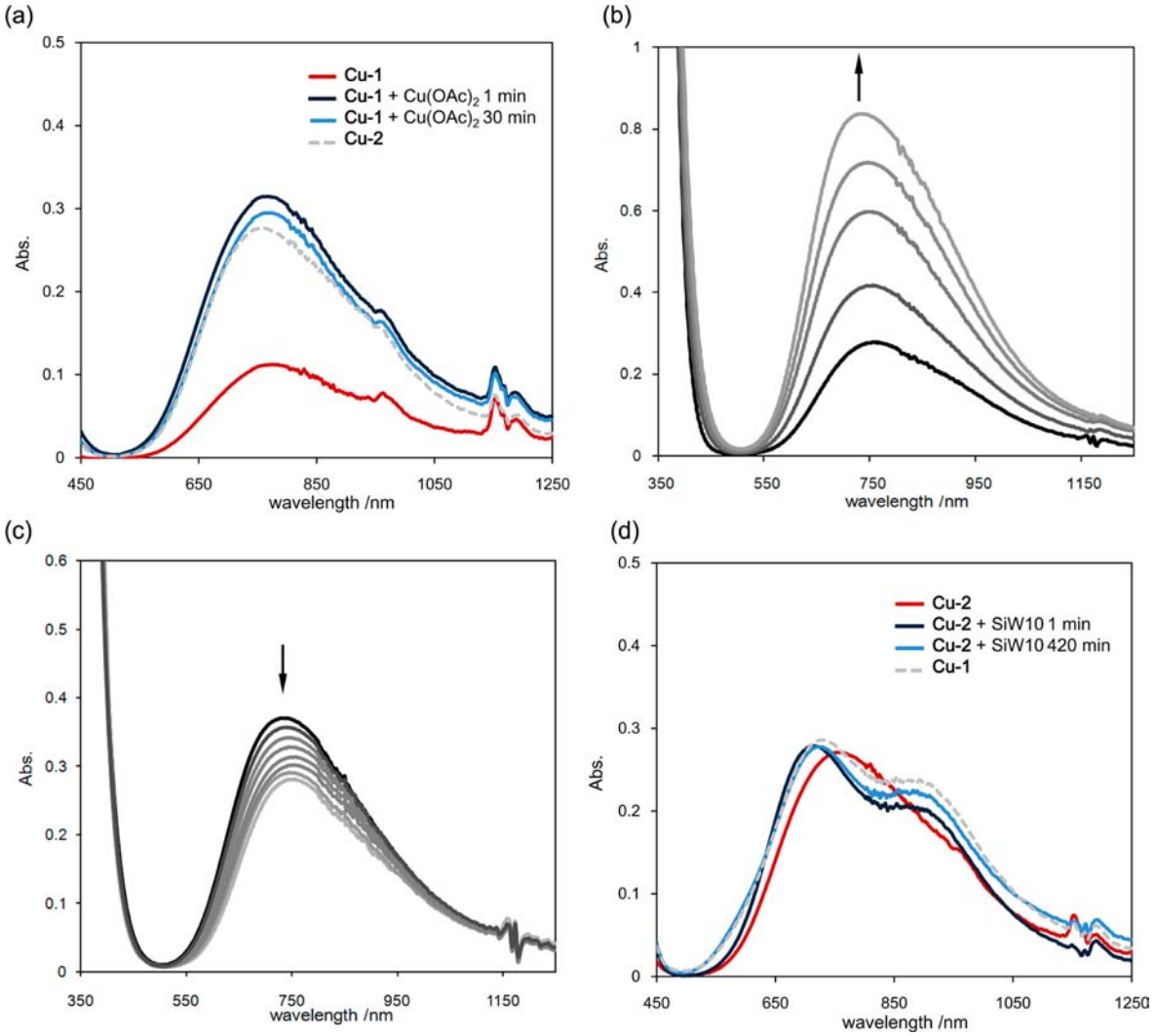

Figure 6. UV−vis spectra of (a) **Cu-1** treated with 1.0 equiv of $Cu(OAc)_2$ (acetonitrile/water, 20:1 v/v), (b) **Cu-2** treated with 0.5, 1.0, 1.5, and 2.0 equiv of $Cu(OAc)_2$ (from bottom to top around 750 nm; acetonitrile/water, 40:1 v/v), (c) **Cu-4** treated with 0.25, 0.5, 0.75, 1.0, 1.25, 1.5, 1.75, and 2.0 equiv of SiW10 (from top to bottom around 750 nm; acetonitrile/water, 40:1 v/v), and (d) **Cu-2** treated with 2.0 equiv of SiW10 (acetonitrile/water, 40:1 v/v).

structure was observed in organic solvents such as acetonitrile, acetone, and 1,2-dichloroethane. This is probably because coordination of oxygen atoms of $[\gamma\text{-}SiW_{10}O_{36}]^{8-}$ to axial positions of copper cations is relatively weak and **Cu-4** is easily dissociated into a monomerized structure of $TBA_4H_2[Cu_2(SiW_{10}O_{36})(OH)(CH_3COO)]$ under the conditions of CSI-MS measurements.

BVS values of silicon (3.91−4.05), tungsten (5.58−6.41), and copper (1.88−2.13) atoms in **Cu-1**, **Cu-2**, and **Cu-4** indicate that the respective valences are +4, +6, and +2. X-ray crystallographic analyses, CSI-MS, elemental analyses, and TG-DTA show that the formulas of **Cu-1**, **Cu-2**, and **Cu-4** are $TBA_8[Cu(\gamma\text{-}SiW_{10}O_{34})_2(CH_3CONH)_2]\cdot 4H_2O$, $TBA_8H_4[Cu_2(\gamma\text{-}SiW_{10}O_{36})_2(H_2O)]\cdot 11H_2O\cdot CH_3COCH_3$, and $TBA_8H_2[Cu_4(\gamma\text{-}SiW_{10}O_{36})_2(CH_3COO)_2]\cdot 5H_2O$, respectively. (See the Supporting Information.) Formation of **Cu-1**, **Cu-2**, and **Cu-4** can be expressed by the following eqs 1−3, respectively:

$$Cu^{2+} + 2[H_4(\gamma\text{-}SiW_{10}O_{36})]^{4-} + 2CH_3CONH_2 \rightarrow [Cu(\gamma\text{-}SiW_{10}O_{34})_2(CH_3CONH)_2]^{8-} + 4H_2O + 2H^+ \quad (1)$$

$$2Cu^{2+} + 2[H_4(\gamma\text{-}SiW_{10}O_{36})]^{4-} + H_2O \rightarrow [Cu_2(\gamma\text{-}SiW_{10}O_{36})_2(H_2O)]^{12-} + 8H^+ \quad (2)$$

$$4Cu^{2+} + 2[H_4(\gamma\text{-}SiW_{10}O_{36})]^{4-} + 2CH_3COO^- \rightarrow [Cu_4(\gamma\text{-}SiW_{10}O_{36})_2(CH_3COO)_2]^{10-} + 8H^+ \quad (3)$$

Copper cation(s) in **Cu-1**, **Cu-2**, and **Cu-4** possessed mononuclear square-planar, dinuclear square-pyramidal, and tetranuclear elongated octahedral coordination geometries, respectively, and were different from each other. In addition to the coordination geometries, the environments (e.g., arrangements of copper cations, Cu−O−Cu bridging angles, and Cu···Cu distances) were different from each other. Therefore, we investigated effects of their core structures on magnetic properties (Figure 3). The $\chi_m T$ values at 300 K for **Cu-1**, **Cu-2**, and **Cu-4** were 0.40, 0.70, and 1.56 $cm^3\ mol^{-1}\ K$, respectively, and close to the theoretical spin-only values of 0.37 (one Cu^{2+} ion), 0.75 (two Cu^{2+} ions), and 1.50 (four Cu^{2+} ions) $cm^3\ mol^{-1}\ K$, respectively. The temperature-dependent magnetic susceptibility of **Cu-2** showed that two copper cations in **Cu-2** were weakly antiferromagnetically coupled ($J = -0.41\ cm^{-1}$, Figure 3b), in accord with a large Cu−O−

dx.doi.org/10.1021/ic301488a | Inorg. Chem. 2012, 51, 11574−11581

Cu angle (156.5(4)°) and a long Cu···Cu distance (4.810(4) Å).[20] In contrast, magnetic susceptibility of **Cu-4** with smaller Cu−O−Cu angles (92.6(4)−134.4(6)°) and shorter Cu···Cu distances (2.871(3)−2.872(4) Å) showed that four copper cations were strongly ferromagnetically (J_a = 72 cm^{-1}, Cu1−O−Cu2) and antiferromagnetically (J_b = −112 cm^{-1}, Cu1−O−Cu1*; J_c = −24 cm^{-1}, Cu1−O−Cu2*) coupled (Figure 3c).[21] The ferromagnetic and antiferromagnetic interactions have been reported for copper cations with Cu−O−Cu angles of ∼90° and much larger than 90°, respectively.[22]

Reversible Transformations. Whereas the CSI-MS of **Cu-1** in 1,2-dichloroethane showed only two sets of **Cu-1** signals centered at m/z 7182 and 3713 (Figure 2a), the spectrum in acetonitrile showed a new set of signals centered at m/z 3682 assignable to $[TBA_5H(SiW_{10}O_{34})(CH_3CONH)]^+$ in addition to **Cu-1** signals (Figure 4a). Therefore, we attempted to demonstrate transformation of **Cu-1** to **Cu-2** by addition of $Cu(OAc)_2$ to the acetonitrile solution of **Cu-1**. When 1 equiv of $Cu(OAc)_2$ was added, two sets of **Cu-1** signals weakened, a new set of signals centered at m/z 3803 assignable to $[TBA_5Cu(SiW_{10}O_{34})(CH_3CONH)(CH_3COO)]^+$ appeared, and the signal intensities leveled off within 2 min. No set of **Cu-2** signals appeared even after 2 h (Figure 4b). This is probably because of strong coordination of CH_3CONH to lacunary sites of $[\gamma\text{-}SiW_{10}O_{36}]^{8-}$. By addition of a small amount of water to the resulting acetonitrile solution (acetonitrile/water, 100:1 v/v), only two sets of **Cu-2** signals centered at m/z 7198 and 3720 were observed, indicating transformation of **Cu-1** to **Cu-2** (Figure 4c). Light blue powders were obtained by addition of diethyl ether to the resulting solution, and the IR spectrum was very similar to that of **Cu-2**, supporting the transformation (Figure S1 in the Supporting Information).

When 0.5 equiv of $Cu(OAc)_2$ were added to an acetonitrile solution of **Cu-2**, the CSI-MS rapidly changed within 1 min, and a new set of signals assignable to monomerized **Cu-4** (centered at m/z 3860) appeared and two sets of **Cu-2** signals weakened, indicating formation of **Cu-4** (see Figures 5a and 5b). When $Cu(OAc)_2$ (0.5, 1.0, 1.5, and 2.0 equiv, with respect to **Cu-2**) was stepwise added, the set of **Cu-4** signals strengthened, accompanied by decrease in intensities of the two sets of **Cu-2** signals, and no set of signals assignable to a trinuclear copper-containing POM was observed (Figure S2 in the Supporting Information).[23] Two sets of **Cu-2** signals disappeared and only the set of **Cu-4** signals was observed upon addition of 2.0 equiv of $Cu(OAc)_2$, with respect to **Cu-2** (Figure 5c), showing complete transformation to **Cu-4**.[24] The molar absorption coefficient per copper cation (ε) at the 753 nm-band reached up to 37 L mol^{-1} cm^{-1} by addition of 2.0 equiv of $Cu(OAc)_2$ (acetonitrile/water, 40:1 v/v; Figure 6b). The value was close to that of **Cu-4** (ε 34 L mol^{-1} cm^{-1}). Single crystals were obtained by addition of diethyl ether to the resulting solution. The X-ray crystallographic analysis and IR spectrum of the single crystals revealed that the solid-state structure was identical to that of **Cu-4** (Figure S4 in the Supporting Information).[25] All these results indicate that $Cu(OAc)_2$ quantitatively reacts with **Cu-2** to form **Cu-4**.

In an opposite manner, transformation of **Cu-4** to **Cu-2** was carried out via the addition of SiW10 to an acetonitrile solution of **Cu-4**. When SiW10 (0.5, 1.0, 1.5, 2.0 equiv, with respect to **Cu-4**) was stepwise added, two sets of **Cu-2** signals centered at m/z 7198 and 3720 appeared and strengthened, accompanied by decrease in intensities of the set of **Cu-4** signals centered at m/z 3860 (Figure S5 in the Supporting Information). Through the addition of 2.0 equiv of SiW10, with respect to **Cu-4**, **Cu-4** was completely transformed to **Cu-2**. The band intensity of d−d transition of copper cations decreased with increase in amounts of SiW10 added, and the spectrum became identical to that of **Cu-2** via the addition of 2.0 equiv of SiW10 (acetonitrile/water, 40:1 v/v; Figure 6c), supporting the transformation to **Cu-2**.[26]

Finally, transformation of **Cu-2** to **Cu-1** was carried out by addition of SiW10 to an acetonitrile solution of **Cu-2**. When SiW10 (2 equiv, with respect to **Cu-2**) was added, two sets of **Cu-1** signals centered at m/z 7182 and 3713 appeared and strengthened with time, accompanied by decrease in intensities of two sets of **Cu-2** signals centered at m/z 7198 and 3720 and a set of SiW10 signals centered at m/z 3682 ($[TBA_5H(SiW_{10}O_{34})(CH_3CONH)]^+$; see Figure S6 in the Supporting Information).[27,28] After 6 h, **Cu-2** was completely transformed to **Cu-1**. The UV−vis spectra of the resulting solution became almost identical to that of **Cu-1** (acetonitrile/water, 40:1 v/v; Figure 6d), supporting the transformation to **Cu-1**.

CONCLUSIONS

In conclusion, we selectively synthesized three novel Cu_n-bridged (n = 1, 2, or 4) silicodecatungstate dimers by changing the mixing ratios of $Cu(OAc)_2$ and lacunary silicodecatungstate SiW10. These compounds were isolated and characterized by CSI-MS, crystallographic analyses, elemental analyses, and magnetic susceptibility measurements. In addition, we demonstrated the reversible transformations between three compounds simply by controlling the copper/SiW10 molar ratios in the solutions.

ASSOCIATED CONTENT

Supporting Information

Crystallographic data for **Cu-1**, **Cu-2**, and **Cu-4** in CIF formats. CSI-MS, IR spectra, and ORTEP representations (Figures S1−S11). This material is available free of charge via the Internet at http://pubs.acs.org.

AUTHOR INFORMATION

Corresponding Author

*Tel.: +81-3-5841-7272. Fax: +81-3-5841-7220. E-mail: tmizuno@mail.ecc.u-tokyo.ac.jp.

Notes

The authors declare no competing financial interest.

ACKNOWLEDGMENTS

This work was supported by the Grant-in-Aid for Scientific Research from the Ministry of Education, Culture, Science, Sports, and Technology of Japan (MEXT) and Funding Program for World-Leading Innovative R&D on Science and Technology (FIRST Program).

REFERENCES

(1) (a) Pope, M. T. *Heteropoly and Isopoly Oxometalates*; Springer: Berlin, 1983. (b) Hill, C. L.; Prosser-McCartha, C. M. *Coord. Chem. Rev.* **1995**, *143*, 407−455. (c) Okuhara, T.; Mizuno, N.; Misono, M. *Adv. Catal.* **1996**, *41*, 113−252. (d) Mizuno, N.; Misono, M. *Chem. Rev.* **1998**, *98*, 199−218. (e) Neumann, R. *Prog. Inorg. Chem.* **1997**, *47*, 317−370. (f) Kozhevnikov, I. V. *Chem. Rev.* **1998**, *98*, 171−198. (g) Kozhevnikov, I. V. *Catalysis by Polyoxometalates*; Wiley: Chichester, U.K., 2002. (h) Hill, C. L. In *Comprehensive Coordination Chemistry II*, Vol. *4*; McCleverty, J. A., Meyer, T. J., Eds.; Elsevier Science: New York, 2004; p 679. (i) Mizuno, N.; Yamaguchi, K.; Kamata, K. *Coord. Chem. Rev.* **2005**, *249*, 1944−1956.

(2) Tézé, A.; Hervé, G. *Inorg. Synth.* **1990**, *27*, 85−96.

(3) (a) Putaj, P.; Lefebvre, F. *Coord. Chem. Rev.* **2011**, *255*, 1642−1685. (b) Long, D.-L.; Tsunashima, R.; Cronin, L. *Angew. Chem., Int. Ed.* **2010**, *49*, 1736−1758.
(4) (a) Balzani, V.; Credi, A.; Raymo, F. M.; Stoddart, J. F. *Angew. Chem., Int. Ed.* **2000**, *39*, 3348−3391. (b) Chakrabarty, R.; Mukherjee, P. S.; Stang, P. J. *Chem. Rev.* **2011**, *111*, 6810−6918.
(5) (a) Kholdeeva, O. A.; Maksimov, G. M.; Maksimovskaya, R. I.; Kovaleva, L. A.; Fedotov, M. A.; Grigoriev, V. A.; Hill, C. L. *Inorg. Chem.* **2000**, *39*, 3828−3837. (b) Nomiya, K.; Saku, Y; Yamada, S.; Takahashi, W.; Sekiya, H.; Shinohara, A.; Ishimaru, M.; Sakai, Y. *Dalton Trans.* **2009**, 5504−5511. (c) Saku, Y.; Sakai, Y.; Nomiya, K. *Inorg. Chim. Acta* **2010**, *363*, 967−974.
(6) (a) Hathaway, B. J. In *Comprehensive Coordination Chemistry*; Wilkinson, G.; Gill, R. D.; McCleverty, J. A., Eds.; Pergamon Press: New York, 1987; Vol. *5*, Chapter 53. (b) Isele, K.; Franz, P.; Ambrus, C.; Bernardinelli, G.; Decurtins, S.; Williams, A. F. *Inorg. Chem.* **2005**, *44*, 3896−3906.
(7) Examples of copper-containing polyoxometalates: (a) Mialane, P.; Marrot, J.; Rivière, E.; Nebout, J.; Hervé, G. *Inorg. Chem.* **2001**, *40*, 44−48. (b) Kortz, U.; Al-Kassem, N. K.; Savelieff, M. G.; Al Kadi, N. A.; Sadakane, M. *Inorg. Chem.* **2001**, *40*, 4742−4749. (c) Bi, L.-H.; Kortz, U. *Inorg. Chem.* **2004**, *43*, 7961−7962. (d) Reinoso, S.; Vitoria, P.; Felices, L. S.; Lezama, L.; Gutiérrez-Zorrilla, J. M. *Chem.—Eur. J.* **2005**, *11*, 1538−1548. (e) Yamase, T.; Fukaya, K.; Nojiri, H.; Ohshima, Y. *Inorg. Chem.* **2006**, *45*, 7698−7704. (f) Liu, H.; Gómez-García, C. J.; Peng, J.; Feng, Y.; Su, Z.; Sha, J.; Wang, L. *Inorg. Chem.* **2007**, *46*, 10041−10043. (g) Pichon, C.; Mialane, P.; Dolbecq, A.; Marrot, J.; Rivière, E.; Keita, B.; Nadjo, L.; Sécheresse, F. *Inorg. Chem.* **2007**, *46*, 5292−5301. (h) Zhang, Z.; Qi, Y.; Qin, C.; Li, Y.; Wang, E.; Wang, X.; Su, Z.; Xu, L. *Inorg. Chem.* **2007**, *46*, 8162−8169. (i) Kamata, K.; Yamaguchi, S.; Kotani, M.; Yamaguchi, K.; Mizuno, N. *Angew. Chem., Int. Ed.* **2008**, *47*, 2407−2410. (j) Luo, Z.; Kögerler, P.; Cao, R.; Hill, C. L. *Polyhedron* **2009**, *28*, 215−220.
(8) (a) Mal, S. S.; Bassil, B. S.; Ibrahim, M.; Nellutla, S.; van Tol, J.; Dalal, N. S.; Fernández, J. A.; López, X.; Poblet, J. M.; Biboum, R. N.; Keita, B.; Kortz, U. *Inorg. Chem.* **2009**, *48*, 11636−11645. (b) Tan, H.; Chen, W.; Liu, D.; Li, Y.; Wang, E. *Inorg. Chem. Commun.* **2010**, *13*, 1354−1356.
(9) (a) Kamata, K.; Yonehara, K.; Sumida, Y.; Yamaguchi, K.; Hikichi, S.; Mizuno, N. *Science* **2003**, *300*, 964−966. (b) Kamata, K.; Kotani, M.; Yamaguchi, K.; Hikichi, S.; Mizuno, N. *Chem.—Eur. J.* **2007**, *13*, 639−648.
(10) (a) Kikukawa, Y.; Yamaguchi, K.; Mizuno, N. *Angew. Chem., Int. Ed.* **2010**, *49*, 6096−6100. (b) Hirano, T.; Uehara, K.; Kamata, K.; Mizuno, N. *J. Am. Chem. Soc.* **2012**, *134*, 6425−6433. (c) Kikukawa, Y.; Suzuki, K.; Sugawa, M.; Hirano, T.; Kamata, K.; Yamaguchi, K.; Mizuno, N. *Angew. Chem., Int. Ed.* **2012**, *51*, 3686−3690. (d) Suzuki, K.; Sugawa, M.; Kikukawa, Y.; Kamata, K.; Yamaguchi, K.; Mizuno, N. *Inorg. Chem.* **2012**, *51*, 6953−6961. (e) Suzuki, K.; Kikukawa, Y.; Uchida, S.; Tokoro, H.; Imoto, K.; Ohkoshi, S.; Mizuno, N. *Angew. Chem., Int. Ed.* **2012**, *51*, 1597−1601.
(11) (a) *CrystalClear 1.3.6*; Rigaku and Rigaku/MSC: The Woodlands, TX. (b) Pflugrath, J. W. *Acta Crystallogr., Sect, D:* **1999**, *D55*, 1718−1725.
(12) Otwinowski, Z.; Minor, W. Processing of X-ray Diffraction Data Collected in Oscillation Mode. In *Methods in Enzymology*, Carter, C. W., Jr., Sweet, R. M., Eds.; Macromolecular Crystallography, Part A; Academic Press: New York, 1997; Vol. *276*, pp 307−326.
(13) *CrystalStructure 3.8*; Rigaku and Rigaku/MSC: The Woodlands, TX.
(14) Farrugia, L. J. *J. Appl. Crystallogr.* **1999**, *32*, 837−838.
(15) Yadokari-XG, Software for Crystal Structure Analyses, Wakita, K. 2001; Release of Software (Yadokari-XG 2009) for Crystal Structure Analyses, Kabuto, C.; Akine, S.; Nemoto, T.; Kwon, E. *J. Cryst. Soc. Jpn.* **2009**, *51*, 218−224.
(16) Sheldrick, G. M. SHELX97, *Programs for Crystal Structure Analysis*, Release 97-2; University of Göttingen: Göttingen, Germany, 1997.
(17) (i) The ^{1}H NMR spectrum of **Cu-1** in DMSO-d_6 showed signals at 1.75 (CH_3CONH_2), 6.66 (CH_3CONH_2), and 7.27 ppm (CH_3CONH_2), and these chemical shifts were almost same as those of acetamide (1.75 (CH_3CONH_2), 6.68 (CH_3CONH_2), and 7.28 ppm (CH_3CONH_2) in DMSO-d_6). On the other hand, no signal assignable to CH_3COOH was observed (1.91 (CH_3COOH) and 12.0 ppm (CH_3COOH) in DMSO-d_6). (ii) GC analysis of **Cu-1** in acetonitrile showed only the acetamide peak and that of CH_3COOH was not observed. (iii) The CSI-MS of **Cu-1** in 1,2-dichloroethane showed a set of signals centered at m/z 7182 that agree with the pattern calculated for $[TBA_9Cu(SiW_{10}O_{34})_2(CH_3CONH)_2]^+$ (centered at m/z 7182, acetamide coordination) and no signal of $[TBA_9Cu(SiW_{10}O_{34})_2(CH_3COO)_2]^+$ (centered at m/z 7184, acetate coordination) was observed. Therefore, the coordinating ligands in **Cu-1** are assignable to CH_3CONH.
(18) Although elemental analysis and CSI-MS clearly indicated the existence of eight TBA cations per anion, only six cations were observed in the crystallographic analysis. This is because of the severe disordering of the rest two TBA cations.
(19) Nakamoto, K. *Infrared and Raman Spectra of Inorganic and Coordination. Compounds*, 3rd ed.; Wiley−Interscience: New York, 1978; p 233.
(20) The spin exchange Hamiltonian ($H = -2JS_{Cu1}\cdot S_{Cu2}$) was used to fit the magnetic data of **Cu-2** between 1.9−300 K ($J = -0.41$ cm^{-1}, $g = 1.95$, TIP = 5.0×10^{-5} cm^3 mol^{-1}).
(21) The spin exchange Hamiltonian ($H = -2\{J_a(S_{Cu1}\cdot S_{Cu2} + S_{Cu1*}\cdot S_{Cu2*}) + J_bS_{Cu1}\cdot S_{Cu1*} + J_c(S_{Cu1}\cdot S_{Cu2*} + S_{Cu1*}\cdot S_{Cu2}) + J_dS_{Cu2}\cdot S_{Cu2*}\}$) was used to fit the magnetic data of **Cu-4** (J_a, Cu1−O−Cu2 and Cu1*−O−Cu2*; J_b, Cu1−O−Cu1*; J_c, Cu1−O−Cu2* and Cu1*−O−Cu2; J_d, Cu2−O−Cu2*) between 40−300 K ($J_a = 72$ cm^{-1}, $J_b = -112$ cm^{-1}, $J_c = -24$ cm^{-1}, $g = 2.00$, TIP = 6.8×10^{-5} cm^3 mol^{-1}) . (a) Hatfield, W. E.; Inman, G. W. *Inorg. Chem.* **1969**, *8*, 1376−1378. (b) Li, X.; Cheng, D.; Lin, J.; Li, Z.; Zheng, Y. *Cryst. Growth Des.* **2008**, *8*, 2853−2861.
(22) Ruiz, E.; Alemany, P.; Alvarez, S.; Cano, J. *J. Am. Chem. Soc.* **1997**, *119*, 1297−1303.
(23) We attempted to investigate transformation of copper-containing POMs by ^{29}Si and ^{183}W NMR spectroscopies, and no signal was observed because of paramagnetism of the copper cations.
(24) Upon addition of 0.5, 1.0, 1.5, and 2.0 equiv of $Cu(OAc)_2$ with respect to **Cu-2**, the UV−vis spectra show quantitative transformation of **Cu-2** to **Cu-4**, according to Scheme 1 (Figure S3a).
(25) Upon addition of other transition-metal cations such as $Ni(OAc)_3$, $Co(OAc)_2$, $Pd(OAc)_2$, $Rh(OAc)_2$, $Mn(OAc)_3$, and $Ru_3O(OAc)_7$ into acetonitrile solutions of **Cu-2** and **Cu-1**, the CSI-MS of the resulting solutions showed formation of complexed mixtures, indicating that the variable coordination geometries of copper cations is a key for the reversible transformation.
(26) Upon addition of 0.25, 0.5, 0.75, 1.0, 1.25, 1.5, 1.75, and 2.0 equiv of SiW10 with respect to **Cu-4**, the UV−vis spectra show quantitative transformation of **Cu-4** to **Cu-2**, according to Scheme 1 (Figure S3b).
(27) Acetamide was formed in situ by hydration of acetonitrile. Formation of acetamide in the presence of SiW10 has also been reported: Sugahara, K.; Kuzuya, S.; Hirano, T.; Kamata, K.; Mizuno, N. *Inorg. Chem.* **2012**, *51*, 7932−7939.
(28) When SiW10 (2 equiv, with respect to **Cu**-2) and acetamide (4 equiv, with respect to **Cu-2**) were added to the acetonitrile solution of **Cu-2**, two sets of **Cu-1** signals centered at m/z 7182 and 3713 appeared, and a set of SiW10 signals centered at m/z 3682 ($[TBA_5H(SiW_{10}O_{34})(CH_3CONH)]^+$) weakened and did not completely disappeared even after 6 h.